Annals of Pharmacology and Pharmaceutics

Research Article
Published: 25 Jan, 2022

Micromolecular Hydrophilic Extract from Vinegar Baked Radix Bupleuri Affecting Digoxin Distribution by Selectively Inhibiting Pgp Expression

Ya Zhao[1#], Fuwen Xiao[2#], Qiaohong Hu[2] and Ruizhi Zhao[1,3]**

[1]Second Affiliated Hospital, Guangzhou University of Chinese Medicine, China

[2]School of Pharmacy, Guangdong Pharmaceutical University, China

[3]Guangdong Provincial Key Laboratory of Clinical Research on Traditional Chinese Medicine Syndrome, China

[#]These authors are equally contributed to this work

Abstract

Natural products become the focus of modern researchers for developing Pgp inhibitors to Multidrug Resistant (MDR) reverse of Hepatocellular Carcinoma (HCC). Micromolecular Hydrophilic Extract from vinegar baked radix bupleuri (MHE) was reported to inhibit Pgp expression *in vitro* Pgp-over expressing cells. In this paper, we studied the effect of MHE on the *in vivo* behavior of Pgp substrate digoxin to explore its prospect of clinical application as a Pgp inhibitor. Concentrations of digoxin in plasma and tissues were determined by UPLC-MS/MS. Pharmacokinetic parameters were calculated from the plasma concentration–time data by using non-compartmental analysis. The changes of tissue distribution were evaluated by Relative Uptake Efficiency (RUE) and Relative Targeting Efficiency (RTE). The Pgp and Oatp2 mRNA expression in different tissues were determined by qRT-PCR. MHE dose-dependently reduced AUC (0-t), AUC (0-∞), MRT (0-t) of digoxin, and increased its level of CLz/F in rats plasma ($P<0.01$, $P<0.05$). MHE increased RUE of digoxin in liver, but decreased RUE of digoxin in small intestine and plasma. MHE hampering liver Pgp mRNA expression was the main reason of liver-targeting effect. MHE is a potent Pgp inhibitor for multidrug-resistant HCC in clinic for its effect of inhibiting Pgp expression *in vivo* and its liver targeting effect.

Keywords: Micromolecular hydrophilic extract; Vinegar baked radix bupleuri; Pgp inhibitor; Liver-targeting effect; Multidrug resistant; Hepatocellular carcinoma

OPEN ACCESS

Correspondence:

Ruizhi Zhao, Second Affiliated Hospital, Guangzhou University of Chinese Medicine, Neihuan Xilu, Guangzhou Daxuecheng, Guangzhou, 510006, China,

E-mail: 13610241754@163.com

Qiaohong Hu, School of Pharmacy, Guangdong Pharmaceutical University, Waihuan Donglu, Guangzhou, 510006, China,

E-mail: hu_qiaohong@163.com

Received Date: *14 Dec 2021*

Accepted Date: *10 Jan 2022*

Published Date: *25 Jan 2022*

Citation:

Zhao Y, Xiao F, Hu Q, Zhao R. Micromolecular Hydrophilic Extract from Vinegar Baked Radix Bupleuri Affecting Digoxin Distribution by Selectively Inhibiting Pgp Expression. Ann Pharmacol Pharm. 2022; 7(1): 1204.

Introduction

Hepatocellular Carcinoma (HCC), next to lung cancer and gastric carcinoma, ranked as the third deadliest malignant tumor in the world [1]. There were about five hundred thousand HCC patients every year in the world and half of them were Chinese [2]. Surgical was the most effective treatment for early HCC, but chemotherapy was considered as the main comprehensive treatment for middle and advanced HCC and 80% patients belonged to the latter [3,4]. Multidrug resistance is a major clinical obstacle in liver cancer chemotherapy which may be caused by efflux transporters, DNA pairs, autophagy regulation, apoptosis regulation and epigenetic regulation [5,6]. Overexpressing of ATP-Binding Cassette (ABC) efflux transporters is one of the most common mechanisms of MDR.

P-glycoprotein (Pgp), encoded by the ABCB1/mrd1 gene, is one of the best-known ABC transporters with the function of exporting chemotherapy drugs from the inside of cancer cells to the outside, and resulting in intracellular drug accumulation [6,7]. Pgp have been reported to play important roles in inducing MDR in several cancers, such as lung, breast, colon, ovarian cancers and melanomas [6]. Therefore, developing inhibitors of Pgp has become a potential target for treating multidrug resistant cancer. To date, three generation Pgp inhibitors have been discovered, but none of them have been approved for clinical use because of unpredictable side effects or no substantial survival benefits [8-10]. So it's urgent to develop high-efficiency and low-toxicity Pgp inhibitors. Due to the characteristics of low toxicity and higher specificity towards P-gp, natural products become the focus of modern researchers for developing Pgp inhibitors to reverse of MDR [11].

Vinegar Baked Radix Bupleuri (VBRB) is a natural herb which widely applied in traditional Chinese medicine to treat liver-related diseases. Previous study reported that VBRB and Xiao Caihu

Tang (a VBRB representative) had the effect on MDR reversal of hepatocellular carcinoma due to the inhibition effect on Pgp [12,13]. Whether VBRB or its constituents are the ideal Pgp inhibitor needs further study as the mechanism and its material basis are not yet clear.

The Micromolecular Hydrophilic Extract from vinegar baked radix bupleuri (MHE), is the residue of vinegar Bupleuri Radix water extract which the polysaccharides and n-butanol extraction were removed. Our team previously proved that MHE was the effective part of VBRB on liver disease, and could inhibit gene and protein expression of Pgp and increase the uptake of Pgp substrate in Pgp over expressing HEK293 cell [14]. *In vitro* study preliminary revealed that Pgp was the target of MHE. In this paper, we chose the classical Pgp substrate digoxin as model drug, and studied the effect of MHE on the *in vivo* behavior of Pgp substrate for the first time to explore whether MHE could be a potent Pgp inhibitor for clinical use.

Material and Methods

Chemicals and reagents

Digoxin was purchased from Chengdu Herbpurify Co., Ltd (Sichuan, China, batch number: D-077-130904, purity ≥ 98.0%). Ginsenoside Rg1 was obtained from national institutes for food and drug control (Beijing, China, batch number: 0703-2001119, purity ≥ 98.0%). Digoxin tablets were purchased from Shanghai Sine Pharmaceutical Laboratories Co., Ltd (Shanghai, China), vinegar-baked Radix Bupleuri was purchased from Kangmei Medical Company (Guangzhou, China) and the batch number was 150313251 which were identified by Ruizhi Zhao (the corresponding author). Trizol® reagent and M-MLV first strand cDNA synthesis kit were purchased from *in vitro* gen (Carlsbad, US). Power SYRB® Green PCR Master Mix qPCR kit was obtained from thermo scientific (Rockford, US). HPLC grade acetonitrile was purchased from Merck (Darmstadt, Germany). All other Reagents were analytical grade or above from a standard source.

Animals

Adult male Sprague-Dawley rats (250 ± 20 g) were obtained from Guangdong Medical Laboratory Animal Center (certificate NO.: 44007200022740), they were acclimatized in an air conditioned room at 22 ± 2°C for 3 days with a 12 h light and 12 h darkness cycle. All the animals were free to standard laboratory chow and tap water before the experiment. The studies were approved by the animal ethics committee of Guangdong province hospital of traditional Chinese medicine, and the use of animals was carried out in accordance with the guide for the care and use of laboratory animals published by the US National Institutes of Health (NIH Publication no. 85-23, revised 1996).

Preparation and characterization of MHE

100 g VBRB were extracted with 1 L water under reflux twice for 40 min each; thereafter two filtrates were merged and concentrated to 100 mL (1.0 g raw material/ mL). 400 mL Absolute ethanol was added to the concentrated solution and kept for 36 h, then filtered and the supernatant was condensed by removing ethanol. The concentrated water solution was extracted by n-butanol 6 times, and aqueous phase was collected for rotatory evaporation till no n-butanol, and then added water to adjust the concentration to 1 g raw material/mL. MHE was obtained and analyzed by GC-MS and HPLC. The GC-MS analysis was performed with Agilent 78904 GC/5975C inert XL MSD with Triple-Axis Detector (Agilent Technologies, USA). An Agilent 190915-433:325”C capillary (30 μm × 250 μm × 0.25 μm) was used and the flow rate of nitrogen carrier gas was 1.5 mL·min^{-1}, 2.0 μL of samples was inject at a constant temperature of 260°C with split ratio of 30:1. Initial temperature was set at 90°C for 4 min, then steadily rose to 200°C with the rate of 6°C·min-1 and held for 5 min, followed by a ramp to 250°C at 10°C·min^{-1} and maintained for 10 min. MS detection was performed with source temperature at 230°C, electron energy of 70 eV, detection voltage of 1176 V and full scan mode (m/z 50-650). Samples were derived by trimethylsilane before injection into GC-MS. An Agilent 1200 series HPLC system (Agilent Technologies, USA) was used for HPLC analysis. Chromatographic separations were performed on A Diamonsil C18 column (250 mm × 4.6 mm, 5 μm) at 35°C and a gradient elution of water (A), acetonitrile (B) and 0.01M ammonium acetate (C) was programmed as follow: 6% A and 6.5% B at 0 to 35 min, 6% A and 6.5% B - 10% A and 8% B at 35 to 40 min, 10% A and 8% B - 20% A and 10% B at 40 to 45 min, 20% A and 10% B at 45 to 50 min, 20% A and 10% B - 20% A and 30% B at 50 to 65 min, 20% A and 30% B -20% A and 35% B at 65 to 70 min. The flow rate was 1 mL/min and the detection wavelength was 248 nm.

UPLC-MS/MS instrument and condition

Chromatographic analysis was performed on an Accela™ UPLC system (Thermo Fisher Scientific, San Jose, CA). A Hypersil Gold C18 (100 mm × 2.1 mm, 1.9 μm, Thermo Scientific) was employed and the column temperature was 25°C. The mobile phase was composed of (A) water and (B) methanol with the ratio of 30%: 70% for 6 min. The flow rate was 150 μL/min and the injection volume was 5 μL.

Mass spectrometry detection was performed on TSQ Quantum Ultra Triple Quadrupole MS (Thermo Fisher Scientific, San Jose, CA). The ESI source was set in negative ionization mode and the scanning mode was selective reaction mode. The selected monitor ion were m/z:779.29-649.60 for digoxin with collision voltage of 35 eV, m/z:799.29-637.34 for ginsenoside Rg1 with collision voltage of 27 eV. The optimal MS parameters were set with capillary temperature of 350°C, vaporizer temperature of 250°C, sheath gas pressure of 30 Arb, AUX gas pressure of 15Arb, ion sweep gas pressure of 0 Arb and negative polarity of 2500 V.

Preparation of standard solutions and quality control samples

For plasma pharmacokinetic study, the stocking solution of digoxin were prepared in methanol with the concentration of 400 μg/mL and stored at 4°C until use. Calibration standards for plasma samples were prepared by spiking blank rat plasma with appropriate amount of the standard mixture working solutions to obtain final concentrations of 0.156, 0.312, 0.625, 1.25, 2.5, 5, 20, 50 ng/mL. The Quality Control (QC) samples (0.312, 5, 40 ng/mL) were prepared in the same way.

For tissue distribution study, the stocking solution of digoxin were prepared in methanol with the concentration of 500 μg/mL and stored at 4°C until use. Calibration standards for tissue samples were prepared by spiking blank rat plasma with appropriate amount of the standard mixture working solutions to obtain final concentrations of 1.56, 3.12, 6.24, 12.5, 25 and 50 ng/mL for liver and kidney; 1.56, 3.12, 6.24, 12.5, 25, 50 and 100 ng/mL for heart, small intestine and plasma respectively. The Quality Control (QC) samples (3.12, 12.5, 40 or 80 ng/mL) were prepared in the same way.

Sample preparation

120 μL plasma samples were extracted with 10-fold volume of ethyl acetate and vortexed for 30 s, and then centrifuged at 10,000

rpm for 10 min. The supernatant was transferred to a new centrifuge tube and evaporated to dryness under a stream of nitrogen at 40°C. The residue was reconstituted with 135 μL 50% methanol aqueous solution, then 15 μL Rg1 (internal standard, IS) was added and vortexed for 30 s. The mixture was centrifuged 12,000 rpm for 20 min and an aliquot of 5 μL was injected into the UPLC-MS/MS system for analysis.

300 mg of tissue was homogenized with 6-fold volume of 0.9% NaCl and centrifuged the tissue homogenate at 3500 rpm for 15 min. 180 μL supernatant was transferred into a centrifuge tube, then 20 μL Rg1 was added and vortexed for 45 s. The mixture was added to pre-conditioned SPE column, and then eluted with 2 mL of water and 1 mL of methanol gradually. Methanol elution was collected and evaporated to dryness under nitrogen at 40°C. The residue was reconstituted with 60% methanol aqueous solution, thereafter centrifuged 12,000 rpm for 20 min. 5 μL sample was injected into the UPLC-MS/MS system for analysis.

Validation procedures

The specificity was evaluated by comparing blank plasma or blank tissue homogenate, blank plasma or blank tissue homogenate spiked with digoxin and Rg1 and plasma or tissue sample after oral administration of digoxin and MHE. Calibration curves were determined by plotting the peak-area ratios of analyte to IS (Y-axis) *vs.* nominal concentration (X-axis) with 1/x weighted least squares linear regression model. The Lower Limit of Quantification (LLOQ) was determined by spiking the lowest point of calibrator in the blank plasma, at which precision and accuracy should not exceed 20%. The precision and accuracy were estimated by analyzing QC samples with six replicates at low, middle and high concentrations on the same day and on three days respectively. The accuracy was calculated by the ratio of the determined concentration and nominal concentration, and the precision by Relative Standard Deviation (RSD). The extraction recovery was assessed by comparing the peak area of analytes finally obtained from extracted QC samples to those in post-extraction blank samples spiked analytes at the same concentrations. The matrix effect was calculated by comparing the peak area of post-extraction blank samples spiked analytes to those in 50% or 60% methanol aqueous solution. Sample stability was assessed at three QC levels under different storage conditions: at room temperature for 8 h, after three freeze-thaw cycles or at -20°C for 25 days.

Plasma pharmacokinetic study

Digoxin (0.125 mg/kg), digoxin (0.125 mg/kg) - low dose MHE (0.6 g raw material/kg) and digoxin (0.125 mg/kg) - high dose MHE (1.2 g raw material/kg) were orally administrated to SD rats (n=6/group). 400 μL blood samples were collected from orbital plexus of eyes at the designated time points: 0.083, 0.25, 0.5, 1, 2, 4, 6, 8, 10 h. The plasma samples were harvested by centrifugating the blood samples at the speed of 1000 g for 15 min and the supernatant were stored at -20°C until analysis.

Tissue distribution study

Overnight fasted 36 SD rats, randomly divided into 2 groups, were orally administrated digoxin (0.125 mg/kg) or digoxin (0.125 mg/kg)-MHE (0.6 g raw material/kg) respectively. The rats were anesthetized by 10% chloral hydrate (4 mL/kg) and sacrificed at designated time points (5 min, 15 min, 3 h). Tissue samples including heart, liver, kidney and small intestine were harvested and rinsed with ice-cold 0.9% NaCl then blotted dry with filter paper and stored at -80°C.

Quantitative real time PCR analysis

Tissues were homogenized by Trizol reagent to obtain total RNA according to the manufacture's instruction. The first strand cDNA was synthesized by 1 μg of total RNA as template using M-MLV First Strand cDNA Synthesis Kit. PCR primers were 5'-ATGAAACTGCCCCACAAATT-3' (forward) and 5'-CTTTCTGTGTCCAAGGC TGA-3' (reverse) for Pgp, 5'-TGAGGCCCCAGGTTCAACCAC -3' (forward) and 5'-ACTAAGCCATTGAAGCCCCCTGA-3' (reverse) for Oatp 2, 5'-ATGATTCTACCCACGGCAAG-3' (forward) and 5'-CTGGAAGATGGTGATGGGTT-3' (reverse) for GAPDH. Power SYRB® Green PCR master mix qPCR kit was used for real time qPCR reaction on an ABI prism TM 7500 real time qPCR system (ABI, US). The reaction conditions were as follows: 50°C for 120 sec, 95°C for 120 sec, 40 cycles at 95°C for 15 sec and 60°C for 60 sec, then 95°C for 15 sec, 60°C for 60 sec and 95°C for 15 sec. Data were normalized by GAPDH expression in each sample and analyzed by using the 2-ΔΔCt method.

Statistical analysis

Results are presented as the mean ± SD. Student's t-test or one-way Analysis of Variance (ANOVA) were used to determine statistical significance either between two or multiple groups, respectively. Differences were considered to be statistically significant when $p<0.05$. Pharmacokinetic parameters were calculated by non-compartmental methods using DAS2.0 pharmacokinetic software. Tissue distribution effect of MHE on digoxin was evaluated targeting efficiency parameters (RUE and RTE) which calculated according to the following equations:

$$RUE = \frac{AUC_{sample}}{AUC_{contol}}$$

$$RTE = \frac{\left(AUC_{tissue} / AUC_{sum}\right)_{sample} - \left(AUC_{tissue} / AUC_{sum}\right)_{control}}{\left(AUC_{tissue} / AUC_{sum}\right)_{control}}$$

Results

MHE characterization

27 Components were identified by GC-MS including 5 oligosaccharides (sucrose, maltose, lactose, mannose disaccharide, gentiobiose), 11 monosaccharides (xylitol, sorbitol, D-glucose, D-mannose, D-glucuronic acid, D-fructose, D-mannitol, sedoheptulose, D- arabinopyranose, D- ribose, D-Galactopyranose), 4 organic acids (acetic acid , malonic acid, succinic acid, fumaric acid) and other components (cetyl alcohol, inositol, cis-13-oleic acid, 11-cis-octadecenoic acid, trans-9-octadecenoic acid , stearic acid, proline) as shown in Figure 1. 19 amino acids were also indentified by HPLC through comparison with standards which included L- aspartic acid (1), L-glutamic acid (2), L-serine (3), L-glycine (4), L-histidine (5), L-threonine (6), L-arginine (7), L-alanine (8), L-proline (9), γ-aminobutyric acid (10), L-cysteine (11), L-tyrosine (12), L-valine (13), L-methionine (14), L-lysine (15), L-isoleucine (16), L-leucine (17), L-phenylalanine (18), L-tryptophan (19) (Figure 2). The peak area of L-arginine accounted for 35% of the total peak area, so it may be one of the effective components of MHE.

Validation of UPLC-MS/MS method

No endogenous interferences were observed at the retention time of digoxin and internal standard (Ginsenoside Rg1) in all conditions (Figure 3). The calibrations were linear over the concentration range of 0.156~50 ng/mL for plasma sample, 1.56 ng/mL to 50 ng/mL for

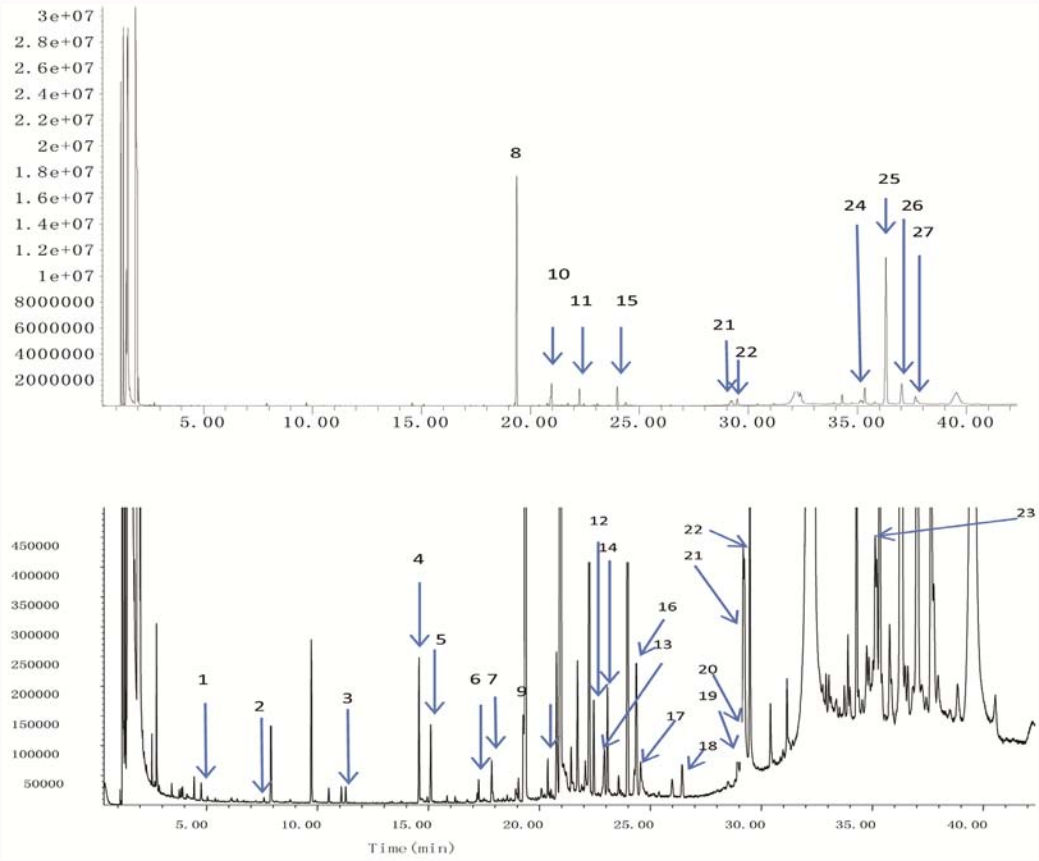

Figure 1: Chemical profile of MHE analyzed by GC-MS. Identification of peaks are as follows: 1, acetic acid; 2, malonic acid; 3, fumaric acid; 4, succinic acid; 5, proline; 6, D- ribose; 7, D-arabinopyranose; 8, xylitol; 9, D-fructose; 10, sorbitol; 11, D-mannose; 12, D-Galactopyranose; 13, sedoheptulose; 14, D-mannitol; 15, D-glucose; 16, D-glucuronic acid; 17, cetyl alcohol; 18, inositol; 19, cis-13-oleic acid; 20, 11-cis-octadecenoic acid; 21, trans-9-octadecenoic acid; 22, stearic acid; 23, mannose disaccharide; 24, gentiobiose; 25, sucrose; 26, maltose; 27, lactose.

Table 1: Results of pharmacokinetic parameters of digoxin after orally administered in rats (n=6).

Parameters		Digoxin		
		Digoxin alone	Digoxin-low dose MHE	Digoxin-high dose MHE
$AUC_{(0-t)}$	ug/L*h	10.89 ± 2.66	7.45 ± 1.80*	6.21 ± 1.53**
$AUC_{(0-\infty)}$	ug/L*h	13.43 ± 2.16	10.09 ± 2.09*	8.56 ± 2.58**
$MRT_{(0-t)}$	h	3.68 ± 0.73	2.80 ± 0.39*	2.76 ± 0.61*
t1/2z	h	3.79 ± 1.23	3.86 ± 1.45	4.01 ± 1.34
Tmax	h	1.20 ± 1.59	1.07 ± 1.65	0.97 ± 1.49
CLz/F	L/h/kg	9.94 ± 1.28	12.88 ± 2.95	15.80 ± 4.90*
Cmax	ug/L	2.46 ± 0.60	2.02 ± 0.42	2.08 ± 0.72

Data represents mean ± SD. *P<0.05 *vs.* Digoxin alone group; ** P<0.01 *vs.* Digoxin alone group

liver and kidney homogenates and 1.56 ng/mL to 100 ng/mL for heart and small intestine respectively with a correlation coefficient (R2) larger than 0.998. The LLOQ of digoxin was 0.156 ng/mL and 1.56 ng/mL for plasma and tissue homogenates respectively. The accuracy were from 85.65% to 114.29% for plasma and from 87.5% to 113.60% for tissue homogenates, while the inter- and intra-day precision (RSD) values were less than 15% for all biological samples. The results indicated the method was accurate and precise. The extraction of digoxin ranged from 70.19% to 98.99% for plasma and from 76.8% to 128.0% for tissue which mean the extraction method was satisfied. The matrix effects were from 96.08% to 114.2% for plasma and from 90.45% to 113.9% for tissue which indicated that no significant matrix effects were observed. Furthermore, the digoxin was stable in rat plasma and various tissue homogenates at room temperature for 8 h, after three freeze-thaw cycles or at -20°C for 25 days.

Effect of MHE on pharmacokinetics of Pgp substrate digoxin

The Mean plasma concentration-time curves of digoxin following oral administration are presented in Figure 4 and pharmacokinetic parameters are shown in Table 1. The data showed that the $AUC_{(0-t)}$, $AUC_{(0-\infty)}$, $MRT_{(0-t)}$ were significantly decreased by 31.54%, 24.92% and 24.42% in digoxin -low dose MHE group when compared to digoxin group (P<0.05), and these significance were much remarkable in digoxin-high dose MHE group by decreasing 42.98%, 36.31%, 21.81%, respectively (P<0.01, P<0.05). Furthermore, MHE increased

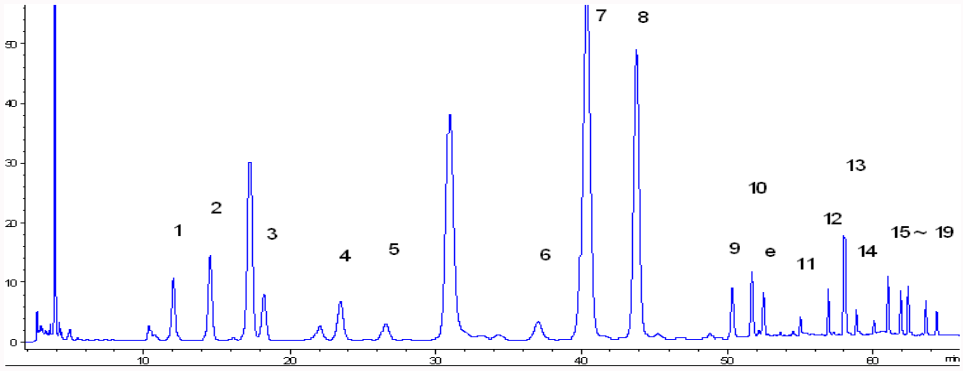

Figure 2: Chromatogram of MHE 1g/mL crude herbal dose by HPLC. 1, L-aspartic acid; 2, L-glutamic acid; 3, L-serine; 4, L-glycine; 5, L-histidine; 6, L-threonine; 7, L-arginine; 8, L-alanine; 9, L-proline; 10, γ-aminobutyric acid; 11, L-cysteine; 12, L-tyrosine; 13, L-valine; 14, L-methionine; 15, L-lysine; 16, L-isoleucine; 17, L-leucine; 18, L-pheylalanine; 19, L-tryptophan.

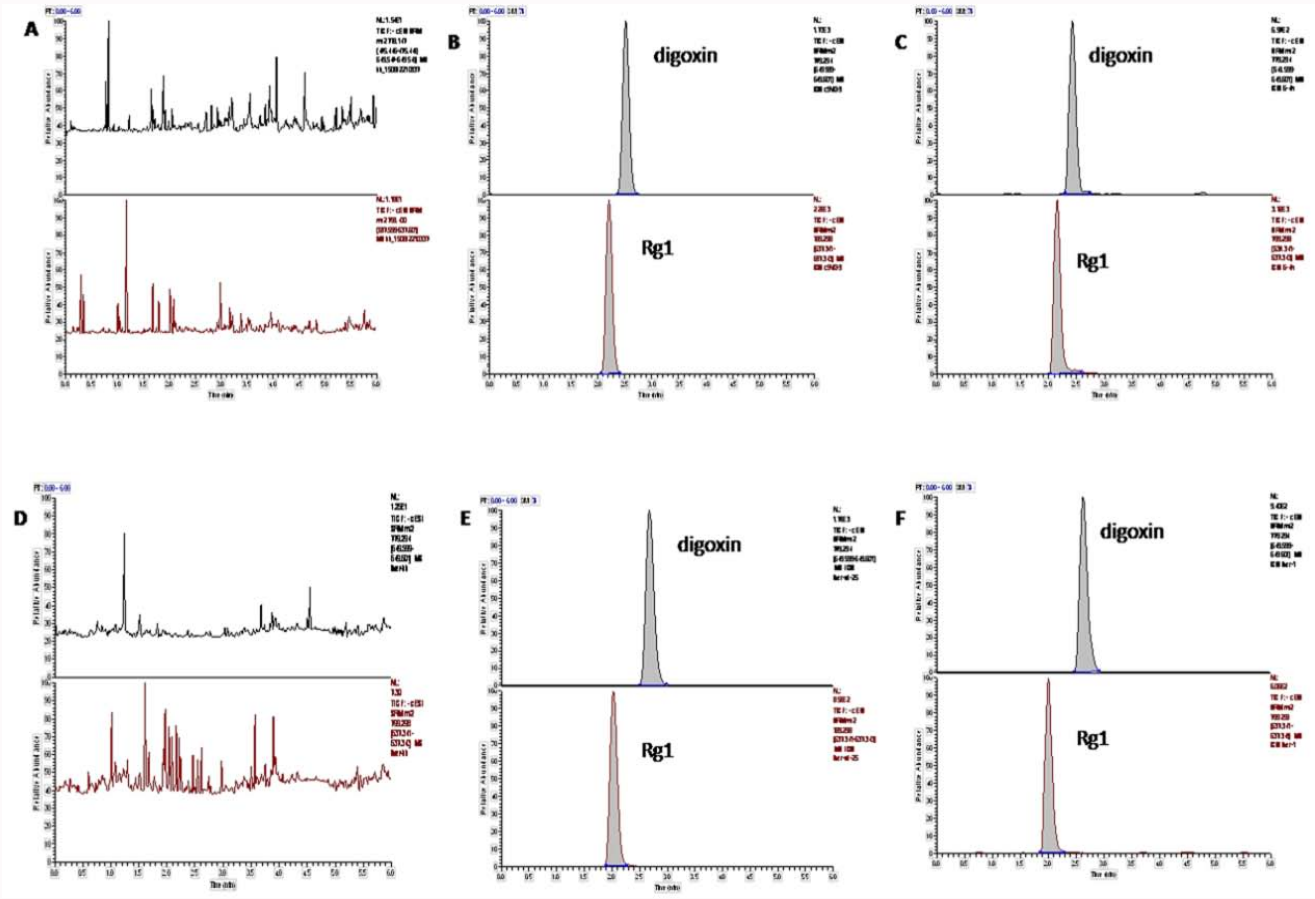

Figure 3: Representative mass spectrum of digoxin and Rg1. (A) Blank plasma sample. (B) Blank plasma sample with digoxin and Rg1. (C) Plasma sample after administration of digoxin and MHE. (D) Blank liver tissue sample. (E) Blank liver tissue sample with digoxin and Rg1. (F) Liver tissue sample after administration of digoxin and MHE.

plasma clearance of digoxin as CLz/F of digoxin increased by 29.6% in digoxin -low dose MHE group and 59.02% in digoxin -high dose MHE ($P<0.05$). Other parameters did not obviously changing between digoxin group and combination group. The results indicated that MHE hampered the absorption of digoxin and promoted its clearance.

Effect of MHE on tissue distribution of P-gp substrate digoxin

The tissue distribution of digoxin in rats after oral administration of digoxin or digoxin-MHE at 5 min, 15 min and 3 h are shown in Figure 5A. In absorption phase (5 min), higher tissue concentrations were observed in digoxin-MHE group than in digoxin group in all tissues analyzed, but all of these differences were insignificant. In equilibrium phase (15 min), the trends were different among different tissues. Compared with digoxin alone group, the concentration of digoxin in liver were remarkably higher ($P<0.05$) in digoxin-MHE group, while digoxin contents in plasma and small intestine significantly decreased ($P<0.05$). In elimination phase (3 h), the tissue concentrations of digoxin were lower in combination group than in

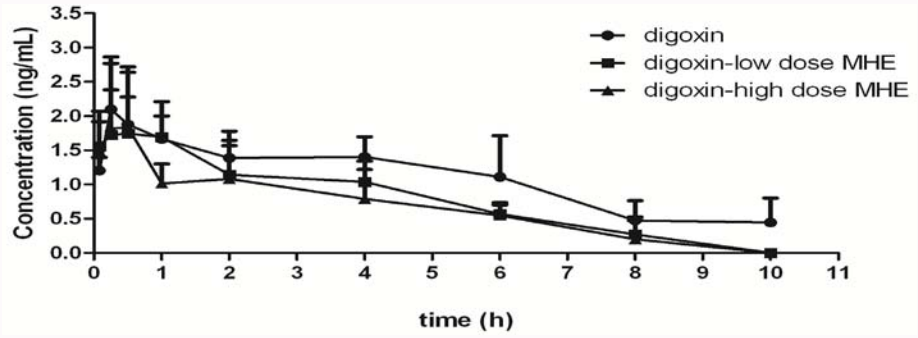

Figure 4: Mean plasma concentration-time curves of digoxin after oral administration of digoxin, digoxin-low dose MHE and digoxin-high dose MHE. Each point represents the mean ± SD of 6 rats.

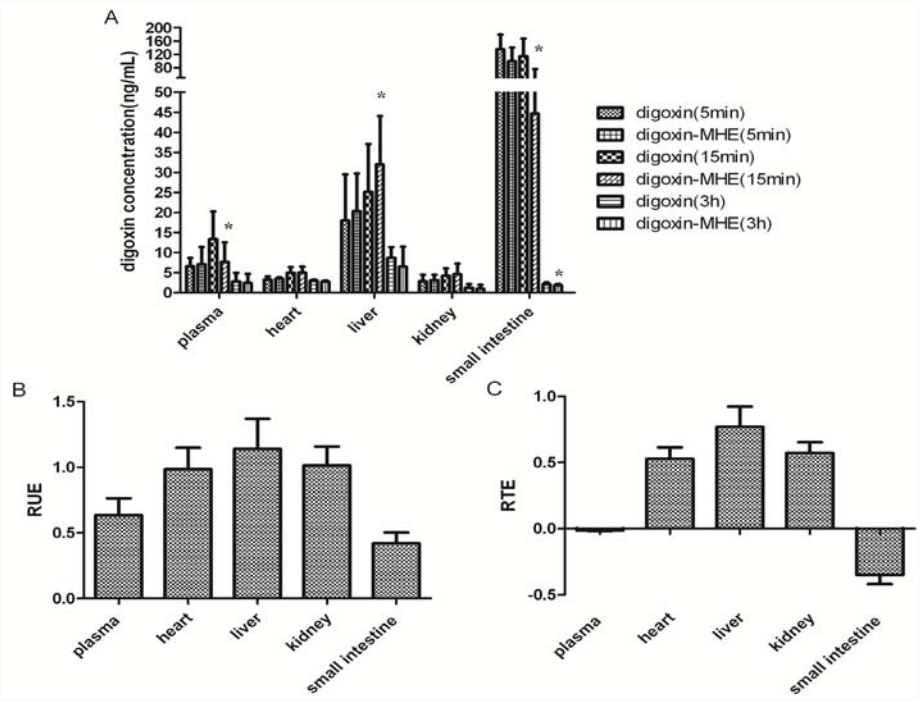

Figure 5: Effect of MHE on tissue distribution of P-gp substrate digoxin. (A) Concentration of digoxin in rat tissues at 5 min, 15 min and 3 h after oral administration of digoxin with or without MHE. (B) RUE of digoxin in different tissues after co-administration with MHE. (C) RTE of digoxin in different tissues after co-administration with MHE *p<0.05 *vs.* digoxin group.

digoxin alone group, and not able difference was observed only in small intestine (P<0.05).

Further, the index of targeting efficiency (RUE and RTE) was use to better evaluated the distribution effect of MHE on digoxin. RUE reflects the effect of MHE on the absorption of digoxin in different tissues. MHE increased the RUE of digoxin in liver by 14.1%, and decreased it in small intestine and plasma by 58.1% and 36.5% respectively. MHE didn't affect digoxin uptake in heart and kidney (Figure 5B). Those indicated that MHE exhibit a liver targeting enhancing effect. RTE is a drug distribution ratio in tissues compared to the control group which related to drug-tissues affinity. A targeting enhancing effect occurs when RTE is above zero, and on the contrary, a targeting weakening effect exhibits. The RTE of heart, liver and kidney were 0.526, 0.769 and 0.571 respectively, while the value was -0.350 in small intestine (Figure 5C). Above results indicated that MHE enhanced the affinity of digoxin with heart, liver and kidney, and the targeting effects were liver > kidney > heart. However, MHE decreased the affinity of digoxin with small intestine.

MHE hampered Pgp gene expression in liver and kidney of rats and enhanced Pgp gene expression in small intestine

Digoxin was the substrate of Pgp and Oatp2 [15], so both transporters were studied to explore the mechanism of *in vivo* behavior change. As shown in Figure 6A, Pgp gene expression decreased in liver after oral administration of digoxin-MHE at 5 min, 15 min and 3 h when compared to administration of digoxin alone, and the difference was significant at 5 min after oral administration (P<0.05). Pgp gene expression was also reduced in kidney obviously in digoxin-MHE group at 5 and 15 min when compared to digoxin group (P<0.01, P<0.05) (Figure 6C). However, MHE significantly increased Pgp gene expression in small intestine at 3 h time point (P<0.05), and it had no obvious effect on Pgp expression in heart (Figure 6E, 6G). As shown in Figure 6B, 6D, liver Oatp2 mRNA expression significantly increased, while kidney mRNA expression significantly decreased in combination group at 3 h time point (P<0.05). Heart and small intestine Oatp2 mRNA expressions did not change between two groups (Figure 6F, 6H).

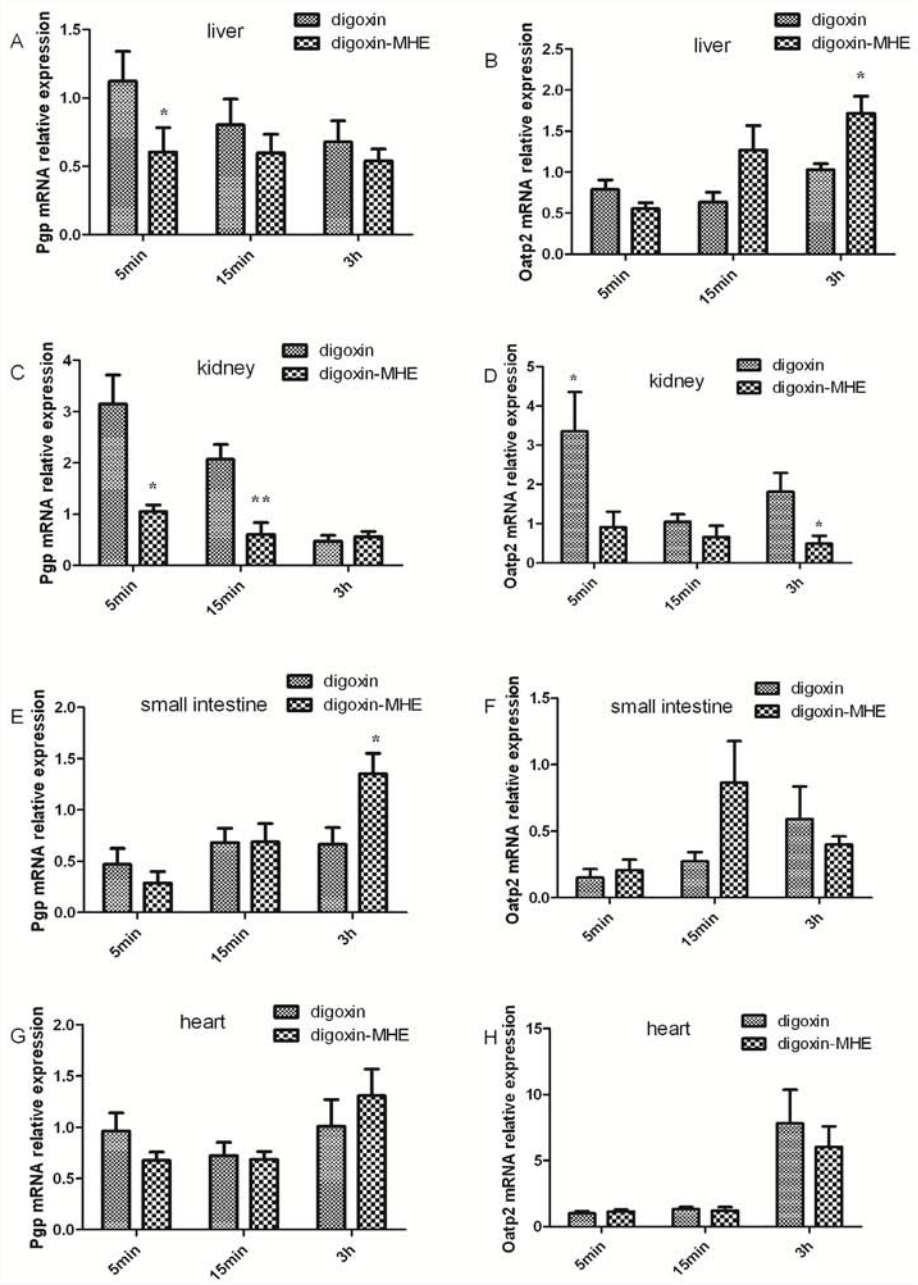

Figure 6: Effect of MHE on Pgp and Oatp2 gene expression in different tissues. After oral administration of digoxin with or without MHE at 5 min, 15 min and 3 h, total RNA extract from different tissues of rats were subject to reverse transcription reaction and qPCR analyses on the Pgp mRNA expression in liver (A), kidney (C), small intestine (E), heart (G) and Oatp2 mRNA expression in liver (B), kidney (D), small intestine (F), heart (H). *p<0.05, **p<0.01 *vs.* digoxin group.

Discussion

MDR is a bottleneck of successful clinical chemotherapy in the treatment of hepatocellular carcinoma. Pgp is one of those key targets as over-expression of P-gp leads to accelerated efflux of chemotherapeutic agents then resulted in the development of MDR. Although many Pgp inhibitors have been discovered to re-sensitize MDR cells when co-administrated with chemotherapeutic agents *in vitro*, none have advanced to the clinic [15,16]. The main mechanism of P-gp inhibitors is competition for binding sites of chemotherapeutic agents, but multiple binding sites on P-gp makes it much difficult to design targeted inhibitors. Developing Pgp inhibitors from natural products with the properties of high-specific but following different mechanism of actions and high-safety became hotspot recent years [17]. Natural herb VBRB was used for MDR of hepatocellular carcinoma in clinic and MHE from VBRB was suggested to be the Pgp inhibitor *in vitro* in our previous study. Thus, the influence of MHE on disposition of P-gp substrate *in vivo* was studied in this paper to explore the potential of developing it as a Pgp inhibitor in clinic.

The results of pharmacokinetic study showed that MHE dose-dependently reduced $AUC_{(0-t)}$, $AUC_{(0-\infty)}$, $MRT_{(0-t)}$ of digoxin in plasma, meanwhile increased its elimination rate. It indicated that MHE hampered the absorption of digoxin and promoted its clearance. Digoxin is not metabolized in the body and 60% to 90% of it was excreted from urine, so small intestinal absorption and renal elimination of digoxin are mainly associated with Pgp [18,19]. Pgp

could accelerate the transport of drug from intestinal epithelial cells, renal tubular cells and liver cells to the nearby lacuna, then expedited drug elimination of these tissues, thus affected drug absorption, distribution, metabolism and excretion [20]. Thus MHE changed pharmacokinetic profile of digoxin may be affected by inhibiting Pgp activity in small intestine, liver, and kidney.

To gain deep insight of MHE effect on Pgp substrate in different tissues, we studied tissue distribution of digoxin when coadministration with MHE. RUE, the relative uptake efficiency, is the index of drug concentration change in tissue of combined group when compared to single group. The results indicated that MHE increased RUE of digoxin in liver, but decreased RUE of digoxin in small intestine and plasma, and it had marginal effect on RUE of digoxin in heart and kidney. Those suggested that the decreased digoxin concentration in small intestine and the increased digoxin concentration in liver might be the cause of the decreased digoxin concentration in plasma. RTE, the relative targeting efficiency, was used for further analysis of the effect of MHE on digoxin relative distribution characteristics in tissues. The RTE of digoxin in small intestine was -0.350 which indicated that MHE hampered the absorption of digoxin. This result was accordance with the pharmacokinetic study that total digoxin concentration was decreased. Under this condition, MHE prompted digoxin distribution to liver, kidney and heart with the RTE of 0.769, 0.571 and 0.526 respectively which may be another reason for the lower plasma concentration of digoxin. As liver and kidney were metabolic and excretory tissues, above results were also accordance with the pharmacological study that MHE could accelerated the clearance of digoxin. Interestingly, although the digoxin plasma concentration was reduced, MHE didn't affect digoxin concentration in heart. So digoxin doses didn't need to be increased when coadministration with MHE in clinic, and digoxin concentration in blood could not reflect its clinical efficacy and toxicity with drug combination treatment.

Drug metabolism enzymes and transporters are the main factors that affect *in-vivo* disposition of drugs [21,22]. Since digoxin is mainly excreted by original type, we hypothesized that drug transporters play a key role on the *vivo* behavior change of digoxin which was affected by MHE. Digoxin is the substrate of both Pgp and Oatp2. So Pgp and Oatp2 gene expression were detected in tissues of single group and combination group to elucidate the mechanism of pharmacokinetic and tissue distribution changes of digoxin affected by MHE. Pgp is ubiquitously expressed in human tissues especially in liver, kidney and small intestine. In the liver, Pgp is mainly expressed in the bile canalicular of hepatocytes and in the apical surface of epithelial cells of small bile ducts with the major function of elimination of drugs and toxins into the bile [17]. When Pgp function is inhibited, the Pgp substrate concentration increased in liver. In this study, Pgp mRNA expression decreased in liver of combination group at 5 min after oral administration. As the effect of gene expression on the drug concentration was delayed, this result was accordance with increased digoxin concentration in liver of combination group at 15 min point in the previous study. So we concluded that MHE hampering Pgp mRNA expression was one of the reasons of increased digoxin concentration in liver. Kidney Pgp is mainly located on the upper surface of epithelial cells of the renal tubule which is responsible for removing xenobiotics *via* urine [23]. Down-regulated Pgp mRNA expression in kidney of combination group at 5 min and 15 min point indicated that MHE could inhibit Pgp gene expression in kidney. It explained why relative kidney targeting effect exhibited under the condition of decreased total concentration in body. Although Pgp mRNA expression increased at 3 h point, it could not be critical influences as digoxin concentration in small intestine at 3 h point was too low. MHE didn't affect Pgp expression in heart.

Oatp2 is mainly expressed in liver and kidney [24,25]. Liver Oatp2 mRNA expression significantly increased, while kidney mRNA expression significantly decreased in combination group at 3 h time point. However, digoxin concentration in liver and kidney 3 h time point were too low to detect or didn't change between single group and combination group, so the changes of Oatp2 mRNA expression in liver and kidney had no significant effect on digoxin concentration in combination group when compared with single group. Furthermore, Oatp2 mRNA expression in heart and small intestine did not change in two groups. As a result, Oatp2 was not the main factor of digoxin tissue distribution change affected by MHE. Selectively inhibiting Pgp expression was the main mechanism that MHE increased liver or kidney targeting of digoxin especially liver targeting. In that case, MHE might be a potent Pgp inhibitor that could be used in clinic for multidrug-resistant HCC. The results needs to be further validated to explore the effect of MHE on Pgp-induced multidrug-resistant HCC model. Furthermore, there were many components in MHE as we analyzed above and most of them were common ingredients in foods. So which components play the Pgp inhibitory effect also needs further research.

In conclusion, MHE was potent Pgp inhibitors for multidrug-resistant HCC in clinic for its effect of inhibiting Pgp expression *in vivo* and its liver targeting effect.

Acknowledgment

This work was generously supported by the National Natural Science Foundation of China (Grant No. 81573612 and 81703798), the Natural Science Foundation of Guangdong Province of China (Grant No. 2015A030313357), Science and Technology Planning Project of Guangdong Province of China (Grant No.2017A020211013).

References

1. Zhou F, Teng F, Deng P, Meng N, Song Z, Feng R. Recent progress of nano-drug delivery for cancer treatment. Anticancer Agents Med Chem. 2018;17(14):1884-97.
2. Wallace MC, Preen D, Jeffrey GP, Adams LA. The evolving epidemiology of hepatocellular carcinoma: A global perspective. Expert Rev Gastroenterol Hepatol. 2015;9(6):765-79.
3. Donadon M, Solbiati L, Dawson L, Barry A, Sapisochin G, Greig PD, et al. Hepatocellular carcinoma: The role of interventional Oncology. Liver Cancer. 2016;6(1):34-43.
4. Kulik L, El-Serag HB. Epidemiology and management of hepatocellular carcinoma. Gastroenterology. 2019;156(2):477-91.e1.
5. Pluchino KM, Hall MD, Goldsborough AS, Callaghan R, Gottesman MM. Collateral sensitivity as a strategy against cancer multidrug resistance. Drug Resist Updat. 2012;15(1-2):98-105.
6. Wu Q, Yang Z, Nie Y, Shi Y, Fan D. Multi-drug resistance in cancer chemotherapeutics: Mechanisms and lab approaches. Cancer Lett. 2014;347(2):159-66.
7. Szakács G, Váradi A, Ozvegy-Laczka C, Sarkadi B. The role of ABC transporters in drug absorption, metabolism, excretion and toxicity (ADME-Tox). Drug Discov Today. 2008;13(9-10):379-93.
8. Binkhathlan Z, Lavasanifar A. P-glycoprotein inhibition as a therapeutic approach for overcoming multidrug resistance in cancer: Current status and future perspectives. Curr Cancer Drug Targets. 2013;13(3):326-46.

9. Gandhi L, Harding MW, Neubauer M, Langer CJ, Moore M, Ross HJ, et al. A phase II study of the safety and efficacy of the multidrug resistance inhibitor VX-710 combined with doxorubicin and vincristine in patients with recurrent small cell lung cancer. Cancer. 2007;109(5):924-32.

10. Kelly RJ, Draper D, Chen CC, Robey RW, Figg WD, Piekarz RL, et al. A pharmacodynamic study of docetaxel in combination with the P-glycoprotein antagonist tariquidar (XR9576) in patients with lung, ovarian, and cervical cancer. Clin Cancer Res. 2011;17(3):569-80.

11. Lopez D, Martinez-Luis S. Marine natural products with P-glycoprotein inhibitor properties. Mar Drugs. 2014;12(1):525-46.

12. Gai XD, Zeng CQ, Hong M. Effect of Bupleurm Chinese DC (BCDC) on the MDR reversal of hepatocellular carcinoma and related mechanism. Chem Res Chin Universities. 26:1446-50.

13. Zhang YX, Li CH, Song WG, Jiang L. Effect of Xiao Chaihu Tang on MDR reversal of hepatocellular carcinoma. Qiu Yi Wen Yao. 11(1):486-7.

14. Feng LM, Zhang X, Zhao RZ. Micromolecular hydrophilic extract from vinegar-baked radix bupleuri weakens Pgp efflux function in HEK293-Pgp cells. Chin Pharm Bulletin. 29(12):1684-8.

15. Kaye SB. Reversal of drug resistance in ovarian cancer: Where do we go from here? J Clin Oncol. 2008;26(16):2616-8.

16. Seiden MV, Swenerton KD, Matulonis U, Campos S, Rose P, Batist G, et al. A phase II study of the MDR inhibitor biricodar (INCEL, VX-710) and paclitaxel in women with advanced ovarian cancer refractory to paclitaxel therapy. Gynecol Oncol. 2002;86(3):302-10.

17. Dewanjee S, Dua TK, Bhattacharjee N, Das A, Gangopadhyay M, Khanra R, et al. Natural products as alternative choices for P-glycoprotein (P-gp) inhibition. Molecules. 2017;22(6):871.

18. Drescher S, Glaeser H, Mürdter T, Hitzl M, Eichelbaum M, Fromm MF. P-glycoprotein-mediated intestinal and biliary digoxin transport in humans. Clin Pharmacol Ther. 2003;73(3):223-31.

19. Mikkaichi T, Suzuki T, Onogawa T, Tanemoto M, Mizutamari H, Okada M, et al. Isolation and characterization of a digoxin transporter and its rat homologue expressed in the kidney. Proc Natl Acad Sci U S A. 2004;101(10):3569-74.

20. Marzolini C, Paus E, Buclin T, Kim RB. Polymorphisms in human MDR1 (P-glycoprotein): Recent advances and clinical relevance. Clin Pharmacol Ther. 2004;75(1):13-33.

21. Shi S, Li Y. Interplay of drug-metabolizing enzymes and transporters in drug absorption and disposition. Curr Drug Metab. 2014;15(10):915-41.

22. Shitara Y, Horie T, Sugiyama Y. Transporters as a determinant of drug clearance and tissue distribution. Eur J Pharm Sci. 2006;27(5):425-46.

23. Naud J, Michaud J, Beauchemin S, Hébert MJ, Roger M, Lefrancois S, et al. Effects of chronic renal failure on kidney drug transporters and cytochrome P450 in rats. Drug Metab Dispos. 2011;39(8):1363-9.

24. Liu T, Li Q. Organic anion-transporting polypeptides: A novel approach for cancer therapy. J Drug Target. 2014;22(1):14-22.

25. Kodawara T, Masuda S, Wakasugi H, Uwai Y, Futami T, Saito H, et al. Organic anion transporter oatp2-mediated interaction between digoxin and amiodarone in the rat liver. Pharm Res. 2002;19(6):738-43.